

**投稿論文 (英文)**  
**PAPERS**

# THE APPLICATION OF KOSLOFF AND FRAZIER'S HOURGLASS CONTROL METHOD IN NONLINEAR ANALYSIS

Guoxiong YU<sup>1</sup> and Tadaaki TANABE<sup>2</sup>

<sup>1</sup>Member of JSCE, Dr. of Eng., Research Associate, Dept. of Civil Eng., Nagoya University (Furocho 1, Chikusa-ku, Nagoya 464-01, JAPAN)

<sup>2</sup>Member of JSCE, Dr. of Eng., Professor, Dept., of Civil Eng., Nagoya University

In finite element analysis, a kind of instability, which is called the hourglass mode, arises when one-point quadrature integration rule is used to calculate the stiffness matrix for the 2-D quadrilateral element. To control the instability, various kinds of methods have been proposed, among them, the one proposed by Kosloff and Frazier<sup>1)</sup> is thought to be the most effective and simple one, but in their paper, they confined the hourglass control method within the elastic problems. In this paper, the details of how to apply the hourglass control method in nonlinear analysis is presented, and a modified scheme is proposed to obtain the accurate nonlinear element response.

*Key Words : hourglass control, nonlinear analysis, finite element*

## 1. INTRODUCTION

It has been known for long time that one-point quadrature integration rule provides tremendous benefits in finite element algorithms because the number of evaluations of the semidiscretized gradient operator, commonly known as the [B] matrix, and the constitutive equations, is reduced substantially. For example, in two dimensions fully quadrature integration rule generally requires 4 quadrature points, while in three dimensions, it requires 8 quadrature points. Also studies suggest that the rate of convergence of one-point quadrature element is comparable to that of fully integrated elements.

However, the use of one-point quadrature integration rule results in certain hourglass modes, or zero-energy modes. The term "zero-energy mode" refers to a nodal displacement vector  $\{\mathbf{u}\}$  that is not a rigid-body motion but nevertheless produces zero strain energy  $\{\mathbf{u}\}^T [\mathbf{K}] \{\mathbf{u}\} / 2$ , where [K] is the up-dated stiffness matrix. If a mesh is consistent with a global pattern of these modes, they will quickly dominate and destroy the solution.

Some methods have been proposed to remedy this phenomenon. These methods include the ones proposed by Kosloff and Frazier<sup>1)</sup>, Belytschko and Kennedy<sup>2)</sup> and Flanagan and Belytschko<sup>3)</sup>. The method proposed by Kosloff

and Frazier has been thought to be the most effective one when the rectilinear element is used.

In Kosloff and Frazier's paper, a simple scheme was proposed to control hourglass instabilities by adding an hourglass response matrix to a one-point quadrature stiffness matrix, and it was also shown that for two-dimensional rectilinear elements the element is identical to the incompatible element introduced by Wilson et al.<sup>4)</sup> However, in Kosloff and Frazier's paper, nothing was included in the scope of nonlinear analysis.

In finite element method for nonlinear analysis, there are two places, where the integration rule is used, one is in calculating the tangential stiffness matrix and the other is in calculating the residual force vector of the element.

This paper can be treated as a complement to or extension of Kosloff and Frazier's paper by applying their hourglass control method in nonlinear analysis. In section 2, the derivation of hourglass control method, which is different from the one presented by Kosloff and Frazier's paper but has the same result, is shown, and then in section 5, the methods how to apply this hourglass control method in nonlinear analysis are described (how to obtain the tangential stiffness matrix, how to calculate the stresses and strains inside the element and how to evaluate the residual force vector). Finally, in section 7, the nonlinear response results, which are obtained by the method

developed in section 5, are compared with those by use of the incompatible element. It is found that when element has stronger pure bending modes (this is often the case of thin structure), there will be great difference between nonlinear response results obtained by the method developed in section 5 and those obtained by the incompatible element. To solve this problem, in section 6, a modified scheme is proposed to obtain the accurate response of the structure in nonlinear region when the element has stronger pure bending modes.

Just as pointed out by Kosloff and Frazier, the scheme in this paper appears to be relatively economical in computation and has an added bonus of accurately representing flexural modes of deformation. Moreover, the scheme can be applied in the finite element with a discontinuous displacement field to solve the problem of strain localization with more simplicity and efficiency than the other integration rule<sup>5)</sup>.

In section 5, the identity between the tangential stiffness matrix obtained by hourglass control method and that obtained by the incompatible element with full integration is shown. Therefore, the method described in this paper can not be used to solve the element locking phenomenon when the material tends to become incompressible<sup>6)</sup>.

The discussions of this paper are confined within the rectilinear element. The research for a more general case will be presented in the future publications.

## 2. HOURGLASS CONTROL METHOD IN ELASTIC ANALYSIS

A more clear way of derivation of hourglass control method, which is different from the one presented by Kosloff and Frazier's paper but has the same result, is shown as follows.

Fig.1 shows the eight independent displacement modes of a four-node plane element. The strain energy in an element  $U_e$  can be expressed as:

$$\begin{aligned} U_e &= \frac{1}{2} \{\mathbf{u}\}^T [\mathbf{K}] \{\mathbf{u}\} \\ &= \frac{1}{2} \{\mathbf{u}\}^T \int_{v_e} [\mathbf{B}]^T [\mathbf{D}] [\mathbf{B}] dv \{\mathbf{u}\} \\ &= \frac{1}{2} \int_{v_e} \{\boldsymbol{\epsilon}\}^T [\mathbf{D}] \{\boldsymbol{\epsilon}\} dv \end{aligned} \quad (1)$$

where  $\{\mathbf{u}\}$  is the displacement vector,  $[\mathbf{K}]$  is the element stiffness matrix;  $[\mathbf{D}]$  is the material constitutive matrix,  $[\mathbf{B}]$  is the strain matrix,  $v_e$  is

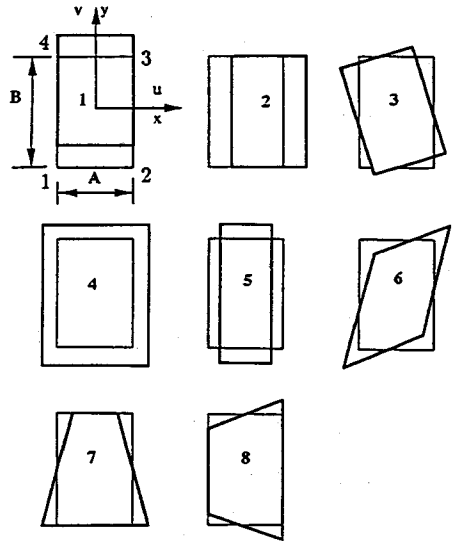


Fig. 1 Independent displacement modes of a four-node plane element

the volume of the element and  $\{\boldsymbol{\epsilon}\}$  is the strain vector.

The first three are rigid-body modes, for which  $U_e = 0$ , as is correct. The next three modes 4,5,6 are constant-strain modes, for which  $U_e > 0$ , regardless of the quadrature integration rule used. Modes 7 and 8 are bending modes. Because at their center,  $\sigma_x, \sigma_y$  and  $\tau_{xy}$  always are zero, according to Eq.(1),  $U_e$  becomes zero when using one-point (center point) quadrature integration rule.

These two modes are called as hourglass modes, because of their shape configurations. These hourglass modes are often a nuisance in numerical calculation when one-point quadrature integration rule is used.

To control these zero-energy modes, restraints are introduced, but at the same time it is required not to affect the element's response to the already existing modes that have already worked well. For simplicity, let us consider only the x-direction nodal displacement  $\{\mathbf{u}_x\}$  of the element shown in Fig.1. For modes 1 and 8, displacements along x direction equal to zero, an arbitrary combination of modes 2 through 7 is

$$\begin{aligned} \{\mathbf{u}_x\} &= \{\mathbf{u}_2\} + \{\mathbf{u}_3\} + \{\mathbf{u}_4\} \\ &\quad + \{\mathbf{u}_5\} + \{\mathbf{u}_6\} + \{\mathbf{u}_7\} \end{aligned}$$

$$\begin{aligned}
&= a_2 \begin{Bmatrix} 1 \\ 1 \\ 1 \\ 1 \end{Bmatrix} + a_3 \begin{Bmatrix} 1 \\ 1 \\ -1 \\ -1 \end{Bmatrix} + a_4 \begin{Bmatrix} -1 \\ 1 \\ 1 \\ -1 \end{Bmatrix} \\
&+ a_5 \begin{Bmatrix} 1 \\ -1 \\ -1 \\ 1 \end{Bmatrix} + a_6 \begin{Bmatrix} -1 \\ -1 \\ 1 \\ 1 \end{Bmatrix} + a_7 \begin{Bmatrix} -1 \\ 1 \\ -1 \\ 1 \end{Bmatrix}
\end{aligned} \quad (2)$$

To provide mode 7 with the stiffness it lacks under one-point quadrature, we add  $[\mathbf{K}]_7$  to the stiffness matrix, where

$$[\mathbf{K}]_7 = \{\mathbf{u}_7\} \{\mathbf{u}_7\}^T \quad (3)$$

By the same way,  $[\mathbf{K}]_8$  can be added to the stiffness matrix computed by one-point quadrature to prevent the mode 8 occurring.

It is possible to choose values of  $a_7$  and  $a_8$  such that a rectangular element displays the exact strain energy in states of pure bending. So in this case

$$a_7 = \left(\frac{E B}{12 A}\right)^{\frac{1}{2}} \quad (4)$$

$$a_8 = \left(\frac{E A}{12 B}\right)^{\frac{1}{2}} \quad (5)$$

where  $A$  and  $B$  are the lengths of the element (Fig.1) and  $E$  is the Young's modulus of the material.

Finally, the hourglass control matrix is obtained as:

$$\begin{aligned}
[\mathbf{K}]_h &= [\mathbf{K}]_7 + [\mathbf{K}]_8 = t \times \\
&\begin{bmatrix} a_7^2 & 0 & -a_7^2 & 0 & a_7^2 & 0 & -a_7^2 & 0 \\ 0 & a_8^2 & 0 & -a_8^2 & 0 & a_8^2 & 0 & -a_8^2 \\ -a_7^2 & 0 & a_7^2 & 0 & -a_7^2 & 0 & a_7^2 & 0 \\ 0 & -a_8^2 & 0 & a_8^2 & 0 & -a_8^2 & 0 & a_8^2 \\ a_7^2 & 0 & -a_7^2 & 0 & a_7^2 & 0 & -a_7^2 & 0 \\ 0 & a_8^2 & 0 & -a_8^2 & 0 & a_8^2 & 0 & -a_8^2 \\ -a_7^2 & 0 & a_7^2 & 0 & -a_7^2 & 0 & a_7^2 & 0 \\ 0 & -a_8^2 & 0 & a_8^2 & 0 & -a_8^2 & 0 & a_8^2 \end{bmatrix}
\end{aligned} \quad (6)$$

where  $t$  is the element thickness.

So in the elastic problems the element stiffness matrix can be obtained as:

$$[\mathbf{K}] = [\mathbf{K}]_{Q4} + [\mathbf{K}]_h \quad (7)$$

where  $[\mathbf{K}]_{Q4}$  is the rectilinear element stiffness matrix calculated by one-point quadrature integration rule.

### 3. NONLINEAR ANALYSIS IN FINITE ELEMENT

The places in nonlinear finite element analysis, where the Gauss quadrature integration rule is used, are briefly shown as follows.

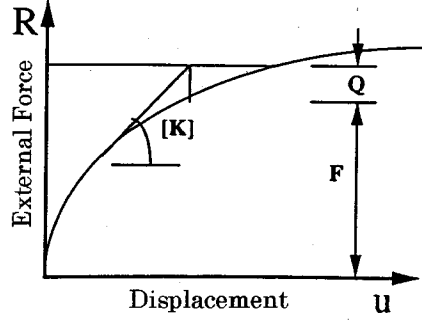


Fig. 2 Nonlinear analysis

There are two places where the Gauss quadrature integration rule is needed. One is when the up-dated element stiffness matrix is calculated, the other is when the vector of residual or so called out-of-balance force is calculated (Fig.2).

Eq.(8) is used to calculate the up-dated stiffness matrix,

$$[\mathbf{K}] = \int_{v_e} [\mathbf{B}]^T [\mathbf{D}_{ep}] [\mathbf{B}] dv \quad (8)$$

where  $[\mathbf{B}]$  is the strain matrix and  $[\mathbf{D}_{ep}]$  is the up-dated constitutive matrix.

The residual force vector can be calculated by using the following equations:

$$\{\mathbf{Q}\} = \{\mathbf{R}\} - \{\mathbf{F}\} \quad (9)$$

$$\{\mathbf{F}\} = \int_{v_e} [\mathbf{B}]^T \{\sigma\} dv \quad (10)$$

where  $\{\mathbf{Q}\}$  is the residual force vector,  $\{\mathbf{R}\}$  is the external force vector,  $\{\mathbf{F}\}$  is the equivalent nodal force vector corresponding to the element stress and  $\{\sigma\}$  is the stress vector of the element.

### 4. INCOMPATIBLE ELEMENT (Q6 ELEMENT)

The incompatible element, which usually is called Q6 element, was firstly introduced by Wilson et al.<sup>(4)</sup> to finite elements in order to enhance their convergence in beam problems.

Now the Q6 element is briefly reviewed. By adding the two bending modes into the Q4 quadrilateral isoparametric element displacement field, it become

$$\mathbf{u} = \sum_{i=1}^4 \mathbf{u}_i N_i(s, t) + \sum_{i=1}^2 \mathbf{a}_i P_i(s, t) \quad (11)$$

where

$$P_1(s, t) = (1 - s^2) \quad (12)$$

$$P_2(s, t) = (1 - t^2) \quad (13)$$

and  $s, t$  are the natural coordinates.

The relation between the strain and the node displacements and interior freedoms are as follows:

$$\begin{Bmatrix} \varepsilon_x \\ \varepsilon_y \\ \gamma_{xy} \end{Bmatrix} = \sum_{i=1}^4 [\mathbf{B}_i] \begin{Bmatrix} u_{xi} \\ u_{yi} \end{Bmatrix} + \sum_{i=1}^2 [\mathbf{G}_i] \begin{Bmatrix} a_{xi} \\ a_{yi} \end{Bmatrix} \quad (14)$$

where

$$[\mathbf{B}_i] = \begin{bmatrix} N_{i,x} & 0 \\ 0 & N_{i,y} \\ N_{i,y} & N_{i,x} \end{bmatrix} \quad (15)$$

$$[\mathbf{G}_i] = \begin{bmatrix} P_{i,x} & 0 \\ 0 & P_{i,y} \\ P_{i,y} & P_{i,x} \end{bmatrix} \quad (16)$$

By using Eq.(8), a  $12 \times 12$  element stiffness matrix can be obtained as

$$\begin{bmatrix} \mathbf{K}^{nn} & \mathbf{K}^{nm} \\ \mathbf{K}^{mn} & \mathbf{K}^{mm} \end{bmatrix} \quad (17)$$

In this stiffness matrix the superscript  $m$  refers to the four new degrees of freedom  $\mathbf{a}_i$  and  $n$  refers to the eight degrees of freedom of the quadrilateral isoparametric element. By condensation<sup>7)</sup>, the  $8 \times 8$  incompatible mode stiffness matrix is given by

$$[\mathbf{K}^{nn}] = [\mathbf{k}^{nn}] - [\mathbf{K}^{nm}][\mathbf{K}^{mm}]^{-1}[\mathbf{K}^{mn}] \quad (18)$$

Stresses and strains are calculated by using all element freedom, including the  $\mathbf{a}_i$ , by Eq.(14). When we use Eqs.(9) and (10) to calculate the residual force,  $\mathbf{a}_i$  will not be included in Eq.(10).

Kosloff and Frazier identified the similarity between the hourglass control method and the Q6 incompatible element. In elastic region, the stiffness matrix obtained by using the hourglass control method(Eqs.(6), (7) and (8)) and that by using the Q6 element are the same.

## 5. HOURGLASS CONTROL METHOD IN NONLINEAR CALCULATION

In section 2, the hourglass control method in elastic analysis has been reviewed and the identity of using the hourglass control method and the Q6 element in elastic region has been proven. However, in inelastic region, some problems of how to apply the hourglass control method still have not been solved. Firstly, when the tangential material constitutive matrix is given, how to apply the hourglass control method described above to obtain the same tangential stiffness matrix as that obtained by Q6 element. Secondly, how to calculate the stresses and strains inside the element. Thirdly, how to calculate the residual force

when the hourglass control method has been used in calculating the tangential stiffness matrix in nonlinear analysis.

In this section, the way to apply the hourglass control method in nonlinear analysis will be developed.

### (1) Tangential Stiffness Matrix

In inelastic region, to obtain the tangential stiffness matrix, values of  $E_x$  and  $E_y$ , which correspond to the up-dated material constitutive matrix  $[\mathbf{D}_{ep}]$  of material, should be substituted into Eqs.(4) and (5), that is:

$$a_7 = \left( \frac{E_x B}{12 A} \right)^{\frac{1}{2}} \quad (19)$$

$$a_8 = \left( \frac{E_y A}{12 B} \right)^{\frac{1}{2}} \quad (20)$$

and then by using the Eqs.(6), (7) and (8), the tangential stiffness matrix can be evaluated.

Supposing the material with the tangential constitutive matrix  $[\mathbf{D}_{ep}]$  is exposed only to the stress increment along x direction, the value of  $E_x$  can be evaluated from the relation between the stress increment of x direction and the resulting strain increment along x direction.

By setting the stress increment vector as:

$$\{\dot{\sigma}\} = (\dot{\sigma}_x, 0, 0)^T \quad (21)$$

and substituting it into the up-dated stress-strain relation, we will obtain

$$[\mathbf{D}_{ep}] \{\dot{\epsilon}\} = \{\dot{\sigma}\} \quad (22)$$

or

$$\begin{bmatrix} D_{11} & D_{12} & D_{13} \\ D_{21} & D_{22} & D_{23} \\ D_{31} & D_{32} & D_{33} \end{bmatrix} \begin{Bmatrix} \dot{\epsilon}_x \\ \dot{\epsilon}_y \\ \dot{\gamma}_{xy} \end{Bmatrix} = \begin{Bmatrix} \dot{\sigma}_x \\ 0 \\ 0 \end{Bmatrix} \quad (23)$$

From the equation above, by Gauss elimination, the second and third terms in the first line of  $[\mathbf{D}_{ep}]$  can be changed to zero. So, the equation of  $\dot{\sigma}_x = E_x \dot{\epsilon}_x$  can be obtained and  $E_x$  can be evaluated. By the same way, by setting  $\{\dot{\sigma}\} = (0, \dot{\sigma}_y, 0)^T$ ,  $E_y$  can be evaluated.

In this research, arbitrary values of  $[\mathbf{D}_{ep}]$  has been assumed. The hourglass control method (Eqs.(6), (7), (8), (19) and (20)) and the Q6 element (Eq.(18)) are used to calculate the stiffness matrix respectively. The two results of the stiffness matrix turn out just to be the same for any arbitrary values of  $[\mathbf{D}_{ep}]$ . This means that the identity of the hourglass control method and the Q6 incompatible element method exists not only in elastic region but also in inelastic region.

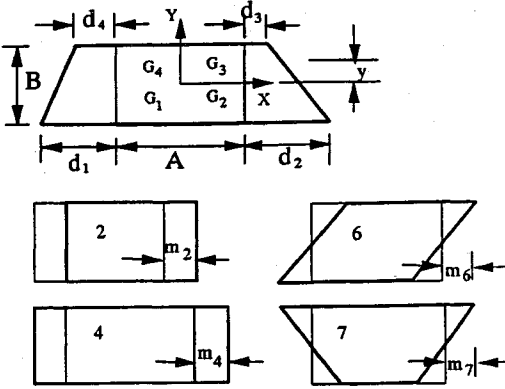


Fig. 3 Strain caused by hourglass mode

## (2) Element Strain and Stress Calculation

When hourglass control method is used, the element stiffness matrix is the same as that when the Q6 incompatible element is used. The same result can be concluded for the element nodal displacements. However, when the strain and displacement relation of Q4 element (Eq.(24)) is used to calculate the strain,

$$\begin{Bmatrix} \varepsilon_x \\ \varepsilon_y \\ \gamma_{xy} \end{Bmatrix} = [\mathbf{B}] \{\mathbf{u}\} = \sum_{i=1}^4 [\mathbf{B}_i] \begin{Bmatrix} u_{xi} \\ u_{yi} \end{Bmatrix} \quad (24)$$

where  $[\mathbf{B}]$  is the same as that in Eq.(14), the strain is correct only at the integration point (where  $t = 0$  and  $s = 0$ ), note that when  $t = 0$  and  $s = 0$ , the strain  $\{\varepsilon\}$  obtained by using Eq.(14) does not include any pure bending modes effect (Fig.1, modes 7 and 8), because at this point  $[\mathbf{G}] = [0]$ .

However, since  $\{\mathbf{u}\}$  is known, it is possible to calculate the strains and stresses caused by hourglass modes (pure bending modes).

For simplicity, let us consider the x direction bending mode. Suppose the element has the nodal displacements along x direction only as in Fig.3, they can be divided into four modes,

modes 2, 4, 6 and 7. So the strains caused by mode 7 at the point at y distance from the x axis will be

$$\varepsilon_{x7} = \frac{y}{BA} (d_1 - d_2 + d_3 - d_4) \quad (25)$$

$$\varepsilon_{y7} = 0 \quad (26)$$

where  $d_i$  ( $i = 1,2,3,4$ ) is the nodal displacement along x direction.

For the same reason, strains caused by mode 8 at the point at x distance from the y axis will be

$$\varepsilon_{x8} = 0 \quad (27)$$

$$\varepsilon_{y8} = \frac{x}{AB} (e_1 - e_2 + e_3 - e_4) \quad (28)$$

where  $e_i$  ( $i = 1,2,3,4$ ) is the nodal displacement along y direction.

The stresses caused by the modes 7 and 8 are

$$\sigma_{x7} = E_x \varepsilon_{x7} \quad (29)$$

$$\sigma_{y7} = 0 \quad (30)$$

$$\sigma_{x8} = 0 \quad (31)$$

$$\sigma_{y8} = E_y \varepsilon_{y8} \quad (32)$$

By adding  $\sigma_{x7}$ ,  $\sigma_{y7}$ ,  $\sigma_{x8}$  and  $\sigma_{y8}$  into the stresses at center point, correct stresses at any point of the element can be evaluated. The above equations are also valid for elastic cases by setting  $E_x = E_y$ .

Actually, the Q6 incompatible element can be derived directly by requiring that the stress variation inside the element be of the form:

$$\sigma_x = C_0 + C_1 y \quad (33)$$

$$\sigma_y = C_2 + C_3 x \quad (34)$$

$$\tau_{xy} = C_4 \quad (35)$$

In hourglass control method, when using Eq.(24) to calculate the strains and the stresses, the stress vector at point  $s = 0, t = 0$  is  $(C_0, C_2, C_4)^T$ .

## (3) The Residual Force

According to Eq.(9), the element stresses are first calculated, and then the equivalent nodal force  $\{\mathbf{F}\}$ , finally the residual force  $\{\mathbf{Q}\}$  can be evaluated. However, as pointed out in section 5.2, using Eqs.(22) and (24) and one-point integration rule, the  $\{\sigma\}$  obtained does not include the stresses caused by modes 7 and 8. The correct equivalent nodal force  $\{\mathbf{F}\}$  of element is the one obtained by Eq.(10) added with the equivalent nodal force  $\{\mathbf{F}_h\}$  caused by modes 7 and 8.

From Eq.(7), we can write

$$([\mathbf{K}]_{Q4} + [\mathbf{K}]_h) \{\mathbf{u}\} = \{\mathbf{R}\} \quad (36)$$

Obviously the equivalent nodal forces caused by modes 7 and 8 are

$$\{\mathbf{F}_h\} = [\mathbf{K}]_h \{\mathbf{u}\} \quad (37)$$

So the equation to evaluate the residual force for hourglass control method is

$$\{Q\} = \{R\} - \{F\} - \{F_h\} \quad (38)$$

where  $\{R\}$ ,  $\{Q\}$  and  $\{F\}$  have the same meaning as in Eqs.(9)(10), and  $\{\sigma\}$  is obtained by using Eqs.(22) and (24). One-point quadrature integration rule is used in Eq.(38).

## 6. COMPARISON BETWEEN THE HOURGLASS CONTROL METHOD AND THE Q6 INCOMPATIBLE ELEMENT IN NON-LINEAR ANALYSIS

The hourglass control method in nonlinear analysis, including the calculation of the tangential stiffness matrix, the stress and strain of the element and the residual force vector have been described in section 5.1 to section 5.3. The nonlinear analysis results by use of the Q6 incompatible element have been proven to be correct in the past, therefore, in this paper, the results obtained by using Q6 incompatible element with full quadrature integration rule are used to check the correctness of the results obtained by the developed hourglass control method in nonlinear analysis.

In the hourglass control method, the one-point (the center point of the element) integration rule is used in evaluation of the element equivalent nodal force. At the center of the element, the stresses, which are the average stresses of the whole element, are used to estimate the nonlinear response of the element. Therefore, when the stronger are the pure bending modes 7 and 8 ( which means the stresses along x and y directions change a lot from one side of the element to the other side of the element, the extreme case is the pure bending of the element), the larger are the difference between the element nonlinear response obtained by using the hourglass control method and those obtained by using Q6 incompatible element method with full quadrature integration rule. This will be shown in numerical examples later in this paper.

To solve the problem of the inaccurate nonlinear response of the element in the case stated above, a modified method is proposed as follows:

1. Use Eq.(7) to evaluate the element stiffness matrix by using one-point quadrature integration rule.
2. Use the equations described in section 5.2 to calculate the stresses at the  $2 \times 2$  Gauss points.

3. Use the stresses at  $2 \times 2$  Gauss points to estimate the nonlinear response of the elements.
4. According to  $\{F\} = \int_{v_e} [B]^T \{\sigma\} dv$ , use the stresses at  $2 \times 2$  Gauss points to calculate the equivalent nodal forces of the element.

In the step 3, when the  $2 \times 2$  Gauss points are used to estimate the nonlinear response of the element, different values of the tangential constitutive matrix  $[D_{ep}]$  of these 4 points can be obtained. By averaging these four  $[D_{ep}]$  and using Eq.(7) to calculate the element stiffness  $[K]$ , the convergence rate will become higher when tangential stiffness method (the element stiffness are recomputed during each iteration of load increment) or combined algorithm (the element stiffness is recomputed for the first iteration of each load increment only) are used in nonlinear analysis.

Although the modified method needs more calculations than the hourglass control method described in section 5 does, compared with the Q4 element, obviously it can reduce calculation time greatly in obtaining stiffness matrix and has the benefit of accuracy of evaluating the bending response of the element. Compared with the Q6 incompatible element, it can reduce calculation time greatly in obtaining the stiffness matrix and the stiffness matrix condensation, while it have the same accurate response in both linear and nonlinear analysis.

## 7. NUMERICAL INVESTIGATION

In this section, numerical proof of the above mentioned algorithm is made in two-dimension nonlinear finite element analysis.

Two groups of example are investigated. The first one is concentrated on one element analysis, the second one is a beam subjected to a transverse external force at the middle of the span. In this section, OPI (one point integration) method denotes hourglass control method developed in section 5, MOPI (modified OPI) method denotes the modified method described in section 6, Q4 element denotes the 4-node quadrilateral element and Q6 element denotes the incompatible element described in section 4.

### (1) Element examination

#### a) Example 1: element subjected to shear force

An element is subjected to shear force. Fig.4 shows the dimension of the element and the external force. The material follows  $J_2$  theory with the material properties : Young's mod-

**Table 1** The stress (kgf/cm<sup>2</sup>) and displacement(cm) in example 1, when  $P = 600\text{kgf}$

		OPI method	Q6 element	Q4 element
Y displacement at point A		$-0.337 \times 10^{-2}$	$-0.337 \times 10^{-2}$	$-0.313 \times 10^{-2}$
Stress at the center of the element	$\sigma_x$	0.00	0.00	
	$\sigma_y$	-60.00	-60.00	
	$\tau_{xy}$	-120.00	-120.00	
Stress caused by hourglass modes at point $G_2$ (Eqs.(29) to (32))	$\sigma_x$	-207.84		
	$\sigma_y$	-103.92		
	$\tau_{xy}$	0.00		
Stress at Gauss point $G_2$	$\sigma_x$	-207.84	-207.84	-163.31
	$\sigma_y$	-163.92	-163.92	-163.92
	$\tau_{xy}$	-120.00	-120.00	-209.08

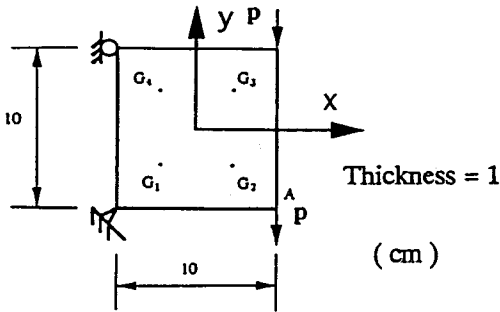


**Fig. 4** Dimension and external force (example 1)

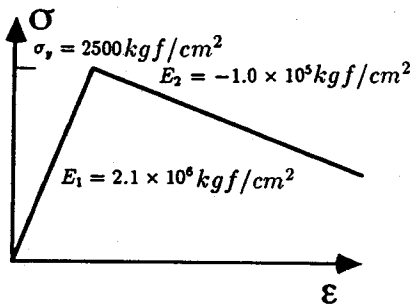


**Fig. 5** Stress-strain relation (example 1)

ulus  $E_1 = 2.1 \times 10^6 \text{kgf/cm}^2$ , plastic modulus  $E_2 = -1.0 \times 10^5 \text{kgf/cm}^2$  and uniaxial yielding stress  $\sigma_y = 2500 \text{kgf/cm}^2$ . The effective stress and effective strain relation is governed by the simple uniaxial test. **Fig.5** shows the assuming stress-strain curve of the material under uniaxial force.

When  $P = 600\text{kgf}$ , the material is in the elastic region. At this time, the stresses at the center of the element and at the  $2 \times 2$  Gauss points and the displacement of point A by using OPI method, Q4 element and Q6 element are shown on **Table 1**, respectively. From the displacement at point A shown in **Table 1**, it can be seen that, OPI method gives the same stiffness as the Q6

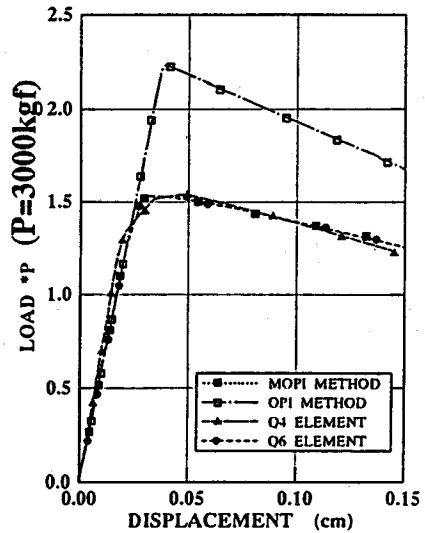


**Fig. 6** Load-displacement curve (example 1)

element, while Q4 element behaves more stiffer than the previous two. For OPI method, stresses at the  $2 \times 2$  Gauss points are calculated by adding the stresses caused by hourglass modes ( Eqs.(29) to (32)) to the stresses at the center point. From **Table 1**, it can be proven that the stresses at the center point and at the  $2 \times 2$  Gauss points by OPI method are the same as those when using Q6 element.

**Fig.6** shows the relation between the load and displacement at point A. In this figure, it can be seen that although the OPI method yields the same result as Q6 element in linear region, there is big difference in nonlinear region, while MOPI method yields almost the same results as Q6 element both in linear and nonlinear region.



**Table 2** The stress (kgf/cm<sup>2</sup>) and displacement(cm) in example 2, when  $P = 600\text{kgf}$

		OPI method	Q6 element	Q4 element
X displacement at point A		$0.171 \times 10^{-2}$	$0.171 \times 10^{-2}$	$0.117 \times 10^{-2}$
Stress at the center of the element	$\sigma_x$	0.00	0.00	
	$\sigma_y$	0.00	0.00	
	$\tau_{xy}$	0.00	0.00	
Stress caused by hourglass modes at point $G_2$ (Eqs.(29) to (32))	$\sigma_x$	207.84		
	$\sigma_y$	0.00		
	$\tau_{xy}$	0.00		
Stress at Gauss point $G_2$	$\sigma_x$	207.84	207.84	148.46
	$\sigma_y$	0.00	0.00	-29.69
	$\tau_{xy}$	0.00	0.00	-59.38

Thickness = 15

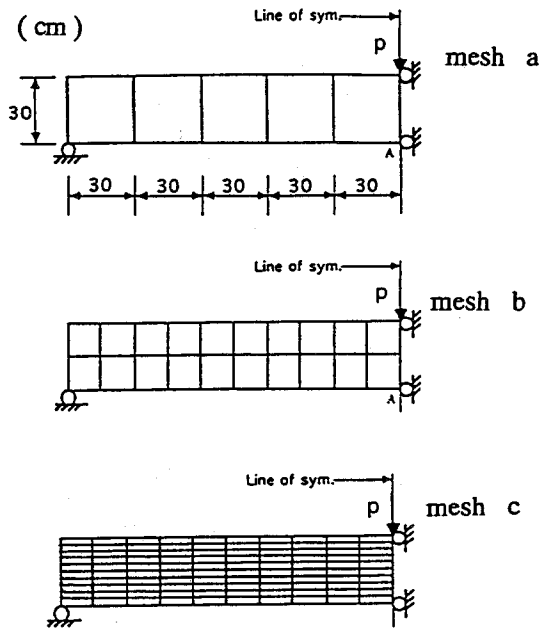
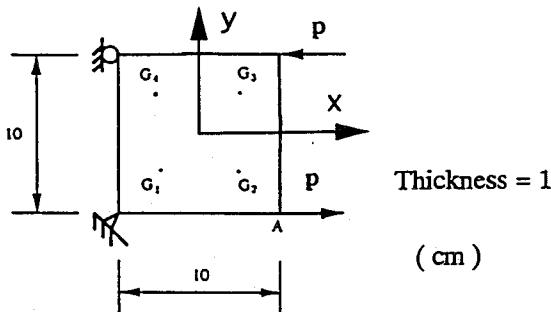


**Fig. 7** Dimension and external force (example 2)

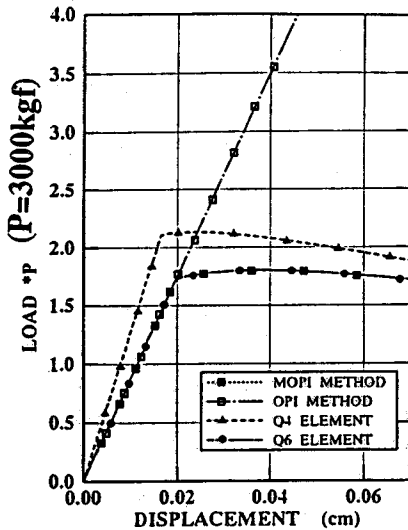


**Fig. 8** Load-displacement curve (example 2)

**b) Example 2: element subjected to pure bending**

The material is the same as in the aforementioned example, but the element is subjected to pure bending force as shown in Fig.7. When  $P = 600\text{kgf}$ , the material is still in linear region,

Table 2 shows the stresses and displacements of the element. The same conclusions for Table 2 can be made as those for Table 1. Fig.8 shows the relation between the load and displacement at point A. In this example, when element is subjected to pure bending, the stresses at the center point are so small that, the material seems never to yield when these stresses are used to evaluate the material nonlinear response (in the case of using OPI method). This can be seen from Fig.8 where the load-displacement curve is a straight line when OPI method is used.

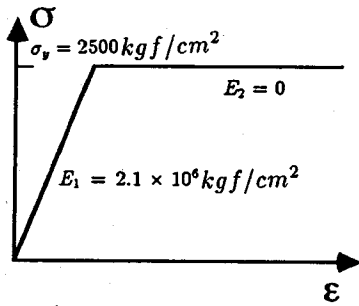


Fig. 10 Stress-strain relation (example 3)

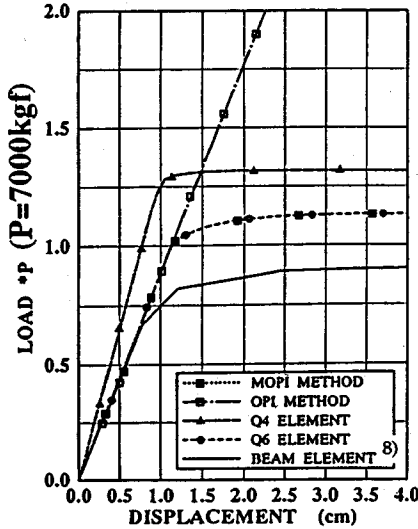


Fig. 11 Load-displacement curve (mesh a)

Table 3 The displacement(cm) at point A for example 3 when P=1400kgf

	OPI method	Q6	Q4
Mesh a	-0.2258	-0.2258	-0.1541
Mesh b	-0.2269	-0.2269	-0.2030
Mesh c	-0.2273	-0.2273	-0.2080

(2) Example 3: beam subjected to a transverse force

A beam is subjected to a transverse external force at the middle of the span. Three types of mesh used to simulate the response of the beam, are shown by Fig.9. Fig.10 shows the material properties with Young's modulus  $E_1 = 2.1 \times 10^6 \text{ kgf/cm}^2$ , plastic modulus  $E_2 = 0$  and the uniaxial yielding stress  $\sigma_y = 2500 \text{ kgf/cm}^2$ . The material is assumed to follow  $J_2$  theory.

When  $P = 1400 \text{ kgf}$ , every elements inside the beam are still in elastic region, the displacements at the middle of the span on bottom side (point

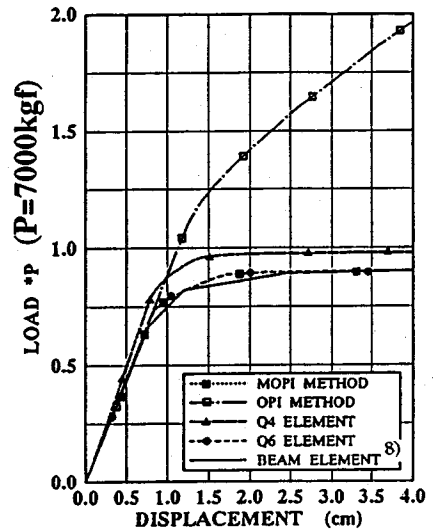


Fig. 12 Load-displacement curve (mesh b)

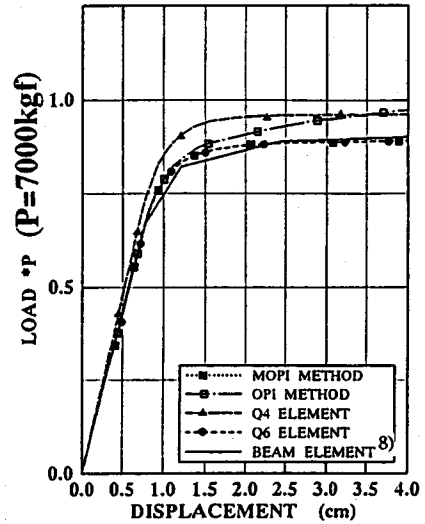


Fig. 13 Load-displacement curve (mesh c)

A) is shown on Table 3. Because OPI method can accurately represent flexural modes of the deformations, even when the mesh with less element(mesh a) is used, rather accurate results can be obtained as shown in Table 3, but Q4 element behaves more stiffer.

Figs.11, 12 and 13 show the relation between the load and displacement at point A by using meshes a, b and c, respectively. When meshes a and b are used, since the pure bending modes of the element are strong, the OPI method gives an inaccurate estimation of the structure nonlinear response (Figs.11 and 12), while a finer mesh (mesh c) is used, the OPI method gives a reasonable result (Fig.13). The reasons of this phe-

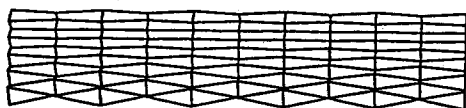


Fig. 14 Deformed mesh  $c$  without hourglass control

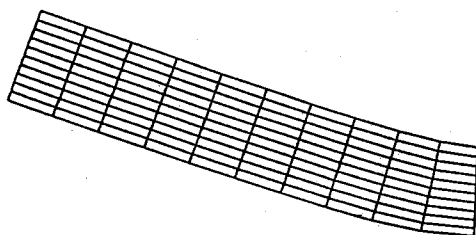


Fig. 15 Deformed mesh  $c$  using MOPI method

nomenon have been stated in section 6. Although the MOPI method needs more calculations than the OPI method does, the MOPI method can give as accurate results as Q6 element does regardless of the mesh used.

Without hourglass control, the nonlinear calculation can seldom be carried on because of the affection of the hourglass modes. Fig.14 shows the deformed mesh  $c$  without hourglass control when very small external force is applied onto the structure. Fig.15 shows the deformed mesh  $c$  when using MOPI method.

## 8. CONCLUSIONS

An hourglass control method in nonlinear analysis, including the calculation of the tangential stiffness matrix, the stresses and strains inside the element and the residual force vector has been described in section 5. Compared with the full quadrature rule, this method can greatly reduce the calculation time in evaluating the tangential stiffness matrix, and the residual force vector. Furthermore, this method has the benefit of accuracy of evaluating the bending response of the element. But when the pure bending modes of the element are strong, this method gives inaccu-

rate nonlinear results compared with those when a full quadrature rule is used. To solve this problem, a modified method has been proposed in section 6. Through numerical examples, it has been proven that although this modified method needs more calculations than the method described in section 5 does, it gives accurate nonlinear results as those when the full quadrature integration rule is used regardless of how cores the mesh is, and can reduce time consumption.

The discussions of this paper are confined within the rectilinear element. The research for a more general case will be presented in the future publications.

## REFERENCES

- 1) Kosloff, D. and Frazier, G.A. : Treatment of Hourglass Patterns in Low Order Finite Element Codes, *Int. J. Num. and Ana. Meth. in Geomechanics*, Vol.2, pp.57-72, 1978.
- 2) Needleman, A. and Tvergaard, V. : Finite Element Analysis of Localization in Plasticity, in: Oden and Garey, eds., *Finite Elements-Special Problems in Solid Mechanics*, Prentice Hall, Englewood Cliffs, NJ, pp.95-297, 1982.
- 3) Flanagan, D.P. and Belytschko, T. : A Uniform Strain Hexahedron and Quadrilateral with Orthogonal Hourglass Control, *Inte. J. Numer. Meths. Engrg.*, Vol.17, pp.679-706, 1981.
- 4) Wilson, E.L. et al. : Incompatible Displacement Models, in: Fenves et al. eds., *Numerical and Computer Methods in Structural Mechanics*, Academic Press, New York, p.43, 1973.
- 5) Yu, Guoxiong, Tanabe, Tadaaki : The Analysis of Localized Failure of Reinforced Concrete Shear Wall *Proceedings of the Japan Concrete Institute*, Vol.17, No.2, pp.1257-1262, 1995.
- 6) Nagtegaal, J.C., Parks, D.M. and Rice, J.R. : On Numerically Accurate Finite Element Solutions in the fully Plastic Range, *Comput. Meths. Appl. Mech. Engrg.*, Vol.4, pp.153-177, 1974.
- 7) Cook, R.D., Malkus, D. and Plesha, M.E. : Concepts and Applications of Finite Element Analysis, *Third Ed.*, John Wiley & Sons, p.193, 1989.
- 8) Owen, D. and Hiton, E. : Finite Elements in Plasticity, Prineridge Press Limited U.K., p.149, 1980.

(Received January 15, 1995)

Kosloff と Frazier によるアワーグラス現象の制御方法における非線形解析の応用

余 国雄・田辺 忠顕

有限要素解析において、アワーグラスという不安定現象がある。それは、一点積分法を用いて、剛性マトリックスを計算する際に生じる。この不安定現象を制御するために、色々な方法が提案されている。その一つである D. Kosloff と G.A. Frazier らによって提案された方法は、長方形要素の場合に、最も有効であり、簡単である。しかし、その方法は、弾性問題に限られる。本論文では、アワーグラス現象制御方法を如何に非線形解析に適用するかの詳細を示している。さらに、より正確な非線形応答を得るために、修正した方法を提案している。